

# Control of Platelet CLEC-2-Mediated Activation by Receptor Clustering and Tyrosine Kinase Signaling

Alexey A. Martyanov,<sup>1,2,3,4</sup> Fedor A. Balabin,<sup>1,2</sup> Joanne L. Dunster,<sup>5</sup> Mikhail A. Pantelev,<sup>1,2,4,6</sup> Jonathan M. Gibbins,<sup>5</sup> and Anastasia N. Sveshnikova<sup>1,2,4,7,\*</sup>

<sup>1</sup>Center for Theoretical Problems of Physico-chemical Pharmacology, Russian Academy of Sciences, Moscow, Russia; <sup>2</sup>Dmitry Rogachev National Medical Research Centre of Pediatric Hematology, Oncology and Immunology, Moscow, Russia; <sup>3</sup>Institute for Biochemical Physics, Russian Academy of Sciences, Moscow, Russia; <sup>4</sup>Faculty of Physics, Lomonosov Moscow State University, Moscow, Russia; <sup>5</sup>Institute for Cardiovascular and Metabolic Research, School of Biological Sciences, Harborne Building, University of Reading, Whiteknights, Reading, United Kingdom; <sup>6</sup>Faculty of Biological and Medical Physics, Moscow Institute of Physics and Technology, Dolgoprudnyi, Russia; and <sup>7</sup>Department of Normal Physiology, Sechenov First Moscow State Medical University, Moscow, Russia

**ABSTRACT** Platelets are blood cells responsible for vascular integrity preservation. The activation of platelet receptor C-type lectin-like receptor II-type (CLEC-2) could partially mediate the latter function. Although this receptor is considered to be of importance for hemostasis, the rate-limiting steps of CLEC-2-induced platelet activation are not clear. Here, we aimed to investigate CLEC-2-induced platelet signal transduction using computational modeling in combination with experimental approaches. We developed a stochastic multicompartmental computational model of CLEC-2 signaling. The model described platelet activation beginning with CLEC-2 receptor clustering, followed by Syk and Src family kinase phosphorylation, determined by the cluster size. Active Syk mediated linker adaptor for T cell protein phosphorylation and membrane signalosome formation, which resulted in the activation of Bruton's tyrosine kinase, phospholipase and phosphoinositide-3-kinase, calcium, and phosphoinositide signaling. The model parameters were assessed from published experimental data. Flow cytometry, total internal reflection fluorescence and confocal microscopy, and western blotting quantification of the protein phosphorylation were used for the assessment of the experimental dynamics of CLEC-2-induced platelet activation. Analysis of the model revealed that the CLEC-2 receptor clustering leading to the membrane-based signalosome formation is a critical element required for the accurate description of the experimental data. Both receptor clustering and signalosome formation are among the rate-limiting steps of CLEC-2-mediated platelet activation. In agreement with these predictions, the CLEC-2-induced platelet activation, but not activation mediated by G-protein-coupled receptors, was strongly dependent on temperature conditions and cholesterol depletion. Besides, the model predicted that CLEC-2-induced platelet activation results in cytosolic calcium spiking, which was confirmed by single-platelet total internal reflection fluorescence microscopy imaging. Our results suggest a refined picture of the platelet signal transduction network associated with CLEC-2. We show that tyrosine kinase activation is not the only rate-limiting step in CLEC-2-induced activation of platelets. Translocation of receptor-agonist complexes to the signaling region and linker adaptor for T cell signalosome formation in this region are limiting CLEC-2-induced activation as well.

**SIGNIFICANCE** C-type lectin-like receptor II-type (CLEC-2) is a recently discovered platelet receptor implicated in the control of vascular integrity. Here, we computationally reconstructed the regulation of tyrosine kinase and calcium signaling network that controls blood platelet activation via CLEC-2 receptor. We demonstrated that the assembly of the receptors in clusters is the rate-limiting processes in the tyrosine-kinase-associated signal transduction, which could explain the slow rates of platelet activation by CLEC-2. Additionally, we demonstrated for the first time, to our knowledge, that CLEC-2 stimulation leads to cytosolic calcium spiking, with a qualitative change caused by the clustering-affecting influences such as temperature and cholesterol saturation.

Submitted November 13, 2019, and accepted for publication April 13, 2020.

\*Correspondence: [agolomy@gmail.com](mailto:agolomy@gmail.com)

Editor: Joseph Falke.

<https://doi.org/10.1016/j.bpj.2020.04.023>

© 2020 Biophysical Society.

## INTRODUCTION

The main task of platelets, nonnucleated cellular fragments produced from megakaryocytes in the bone marrow, is the prevention of blood loss upon vessel wall disruption (1). Platelets circulate in the cardiovascular system for



approximately 7 days until they get eliminated in the spleen or liver (2). Alongside their primary role in hemostasis, platelets have been demonstrated to be involved in angiogenesis (3), tissue remodeling (4,5), and leukocyte recruitment under inflammatory conditions (6,7). Platelets respond gradually to various activators (1). Platelet responses to contact with extracellular matrix protein collagen include shape change, granule release, and, in some cases, cell death (8). In contrast, platelet responses to ADP include only shape change and integrin activation (8).

There are two main types of signaling pathways in blood platelets, associated either with G-proteins or with tyrosine kinase signaling (9). Platelet G-protein-coupled receptors govern responses to ADP (P2Y<sub>1</sub>, P2Y<sub>12</sub> receptors), thromboxane A<sub>2</sub> (TxA<sub>2</sub>), thrombin (protease-activated receptors 1 and 4 (PAR1, PAR4)), epinephrine ( $\alpha$ 2A), and prostacyclin (IP) (10,11). Platelet receptors that induce tyrosine kinase network of signaling are the receptors for collagen (glycoprotein VI (GPVI)) (8,12) and for IgG (Fc $\gamma$ RIIa) (9) and were recently found on platelet receptor C-type lectin-like receptor II-type (CLEC-2) (8). The only confirmed endogenous CLEC-2 ligand is a membrane protein, podoplanin, expressed by the lymphatic endothelial cells (13,14). Therefore, the primary platelet CLEC-2 physiological function is considered to be the separation of blood and lymphatic systems (15–18). Other known CLEC-2 agonists are snake venom protein rhodocytin (19,20) and brown seaweed extract fucoidan (21). CLEC-2 also contributes to the maintenance of blood vessel integrity during inflammatory conditions (17,22–25) and has a role in thrombus formation and wound healing (7,23,26–29) and in various pathologies (30–32). This makes CLEC-2 a prospective therapeutic target (7,29,32,33). Thus, systemic understanding of the CLEC-2 signaling is of essential importance.

A distinct feature observed upon platelet activation via CLEC-2 by either podoplanin, rhodocytin, or fucoidan was 1- to 2-min lag-time before activation (21,34). This has been demonstrated using spectrofluorimetric assay of platelet cytosolic calcium (21). However, it is not understood whether platelet CLEC-2 can induce cytosolic calcium spiking, prolonged cytosolic calcium oscillations, or transient increase of cytosolic calcium. The prolonged platelet CLEC-2-induced response may be a consequence of ADP-containing granule secretion and TxA<sub>2</sub> synthesis. Another possible cause of the significant activation lag-time is the receptor clustering, as was proposed by Pollitt et al. (34). Indeed, glycosylated extracellular stalk regions (35), as well as the GxxxG region in the transmembrane domain of CLEC-2 (35,36), lead to homodimerization of the recombinant CLEC-2 proteins (35). On the surface of the resting platelets, CLEC-2 is present in both dimeric and monomeric forms (35,36). Upon ligand binding, CLEC-2 undergoes multimerization (36), which might be ligand driven (e.g., tetrameric rhodocytin can bind

two copies of single CLEC-2 or two CLEC-2 dimers simultaneously (37)). On the other hand, nonmultimeric podoplanin still induces CLEC-2 cluster formation (38), which implies more complex clustering mechanisms. The platelet responses to CLEC-2 are also highly dependent on actin polymerization and cholesterol presence in the plasma membrane (34,39). However, unlike cholesterol presence, actin cytoskeleton reorganization is not required for CLEC-2 oligomerization (34). Badolia et al. have recently reported that CLEC-2-induced signaling is still detectable after the abrogation of secondary activation (40).

The computational modeling approach could be useful to reveal the sequence of events in CLEC-2-induced platelet activation and identification of rate-limiting steps in this pathway. Mukherjee et al. demonstrated that receptor clustering is significant for the activation of ITAM-bearing receptors (B-cell receptors (BCR) and T cell receptors (TCR)) (41). The significance of platelet receptor clustering was demonstrated experimentally for CLEC-2 (38) and GPVI (42); however, the computational models of GPVI-induced platelet activation do not incorporate the receptor clustering (43,44). Because of their small size, platelets do not possess significant amounts of signaling proteins. For example, there are only 2000 copies of phospholipase C $\gamma$ 2 (PLC $\gamma$ 2) in platelets (~500 nM). Even upon strong activation, no more than 25% of signaling proteins become active (44). Thus, it can be claimed that there are less than 100 active signal-transducing proteins in platelets upon weak stimulation. Because of the low amounts of active participants of the signaling cascades in platelets, deterministic modeling might not be capable of providing reliable calculation results. Thus, stochastic approaches are required for platelet models (45–47).

Here, we aimed to reveal the primary events of platelet activation upon stimulation through CLEC-2 by means of computational modeling and experimental analysis. The proposed *in silico* model described platelet activation starting from ligand binding to CLEC-2 and proceeding until calcium ions release from the dense tubular system. The model predicted that besides tyrosine kinase activity, platelet activation via CLEC-2 is limited by the CLEC-2 receptor clustering in the plasma membrane, the CLEC-2 clustering pattern, and the LAT signalosome formation. Model predictions were supported experimentally by an essential dependence of CLEC-2-induced platelet activation on temperature and by modulation of membrane saturation of cholesterol by methyl- $\beta$ -cyclodextrin (m $\beta$ CD). The model also predicted CLEC-2-induced calcium spiking, which was confirmed experimentally using total internal reflection fluorescence microscopy (TIRF microscopy). Our data enable us to propose a refined concept of signal transduction upon platelet activation via CLEC-2.

## METHODS

### Reagents

The sources of the materials were as follows: calcium-sensitive cell-permeable fluorescent dye Fura-2-AM, Fura Red-AM (Molecular Probes, Eugene, OR), fucoidan from *Fucus vesiculosus*, ADP, PGI<sub>2</sub>, EGTA, HEPES, bovine serum albumin (BSA), apyrase grade VII, and m $\beta$ CD (Sigma-Aldrich, St Louis, MO). VM-64 antibody was a kind gift of Dr. A. V. Mazurov (National Medical Research Centre (NMRC) of Cardiology, Moscow, RF) (48).

### Blood collection and platelet isolation

Healthy volunteers, both men and women aged between 18 and 35 years, were recruited into the study. Investigations were performed under the Declaration of Helsinki, and written informed consent was obtained from all donors. Blood was collected into 4.5 mL tubes containing 3.8% sodium citrate (1:9 vol/vol) and supplemented by apyrase (0.1 U/mL). The study was approved by the Independent Ethics Committee at Center for Theoretical Problems of Physico-chemical Pharmacology, Russian Academy of Sciences (CTP PCP RAS; 1\_2018-1 from 12.01.2018). Platelets were purified by double centrifugation as described previously (45,49). Briefly, platelet-rich plasma was obtained by centrifugation at  $100 \times g$  for 8 min. Platelet-rich plasma was supplemented with additional sodium citrate (27 mM) and centrifuged at  $400 \times g$  for 5 min. The resultant supernatant was removed, and platelets were resuspended in Tyrode's buffer (150 mM NaCl, 2.7 mM KCl, 1 mM MgCl<sub>2</sub>, 0.4 mM NaH<sub>2</sub>PO<sub>4</sub>, 5 mM HEPES, 5 mM glucose, 0.2% BSA (pH 7.4)). Alternatively, blood was collected in Li-heparin (IMPROVACUTER; Guangzhou Improve Medical Instruments Co., China) or hirudin (Monovette; Sarstedt, Newton, NC) containing vacuum tubes.

### Flow cytometry and inhibitory analysis

For continuous flow cytometry experiments, washed platelets were incubated with either 2  $\mu$ M Fura Red-AM (2  $\mu$ M of Fura-2) before the final wash for 45 min at room temperature or for 30 min at 37°C in the presence of apyrase (1 U/mL). Platelets were then incubated in buffer A for 10 min and then centrifuged. Whole blood was incubated with either 2  $\mu$ M Fura Red-AM (or 2  $\mu$ M of Fluo-3 or Fluo-4 and 2  $\mu$ M of Fura-2) for 30 min at 37°C in the presence of apyrase (1 U/mL). Whole blood was diluted 20 times with calcium and albumin containing Tyrode's buffer. Samples were diluted to concentration 1000 pl $\mu$ L and analyzed using FACS Canto II or FACS Aria (BD Biosciences, San Jose, CA) flow cytometer in a continuous regime with 20-s interruption for the addition of an activator.

### Immunoblotting

Human platelets from drug-free volunteers were prepared on the day of the experiment as described previously (50) and suspended in modified Tyrode's-HEPES buffer (134 mM NaCl, 0.34 mM Na<sub>2</sub>HPO<sub>4</sub>, 2.9 mM KCl, 12 mM NaHCO<sub>3</sub>, 20 mM HEPES, 5 mM glucose, 1 mM MgCl<sub>2</sub> (pH 7.3)) to a density of  $1.5 \times 10^9$  cells/mL. Stimulation of platelets with  $10 \times$  fucoidan (final concentration of 1, 10, or 100  $\mu$ g/mL) was performed for 0–15–30–60–90–120–150–180–300 s at 25 or 37°C in an aggregometer with continuous stirring (1000 rpm). Reactions were abrogated by addition of  $4 \times$  sodium dodecyl sulfate-polyacrylamide gel electrophoresis (SDS-PAGE) sample treatment buffer (200 mM Tris-HCl (pH 6.8), b-MeEtOH 400 mM, SDS 4%, bromophenol blue 0.01%, glycerol 40%). Samples were then heated to 99°C for 10 min and centrifuged at  $15,000 \times g$  for 10 min to remove cell debris.

Proteins were separated by SDS-PAGE on 10% gels and transferred to polyvinylidene difluoride membranes that were then blocked by incubation in 5% (w/v) bovine serum albumin dissolved in Tris-buffered saline with Tween 20 (TBS-T). Primary and secondary antibodies were diluted in TBS-T containing

2% (w/v) bovine serum albumin and incubated with polyvinylidene difluoride membranes for 1.5 h at room temperature. Blots were washed four times for 15 min in TBS-T after each incubation with antibodies and then developed using an enhanced chemiluminescence detection system using ECL Prime Western blotting detection reagent. Primary antibodies were used at a concentration of 1  $\mu$ g/mL (anti-phosphotyrosine PY20) or diluted 1:1000 (anti-tubulin). Horseradish-peroxidase-conjugated secondary antibodies were diluted 1:1000. To control for protein loading, membranes were stripped by washing two times for 30 min in stripping buffer (250 mM glycine, 0.2% SDS, 0.1% Tween-20, (pH 2.2)) twice for 10 min in phosphate-buffered saline (PBS) and two times for 5 min in TBS-T at room temperature. Membranes were then blocked for 30 min by 2% TBS-T BSA solution at room temperature and restained with anti-tubulin antibodies.

### Depletion of platelet cholesterol

Cholesterol was depleted from the plasma membrane of platelets by incubation of washed platelets for 15 min with different concentrations of m $\beta$ CD at 37°C before stimulation as described in Mahammad and Pamryd (51).

### Immunofluorescent microscopy

Washed human platelets were activated by fucoidan (100  $\mu$ g/mL) at 25°C (with or without cholesterol depletion by m $\beta$ CD) or at 37°C and fixed by 4% paraformaldehyde (PFA) after 30, 60, 90, 120, and 300 s after activation. Platelets incubated with CRP (5  $\mu$ g/mL) or mQ water for 300 s were used as positive and negative controls, correspondingly. Fixed platelets were washed from PFA by sequential centrifugation, resuspended in PBS-BSA buffer, and adhered to poly-L-lysine (0.1% in mQ; Sigma-Aldrich)-covered glass coverslips for 90 min at 37°C. Nonadherent platelets were removed by gentle rinsing of the coverslips. Fixed platelets on the glass were then permeabilized by 0.2% Triton X-100 in the presence of 2% BSA and 1% goat serum. After permeabilization, platelets were incubated with 1:250 diluted LAT pY1911 (Abcam, Cambridge, MA) antibodies for 90 min at room temperature. After washing primary antibodies off, platelets were incubated with secondary antibodies, conjugated with Fluorescein isothiocyanate (FITC; Imtek, Moscow, RF) for 90 min in the darkroom at room temperature. After washing off secondary antibodies, cells were additionally fixed by adding 4% PFA for 10 min. Samples were then mounted with Dako fluorescence mounting media (Agilent Technologies; Santa Clara, CA). Samples were analyzed by means of Zeiss Axio Observer Z1 microscope (Carl Zeiss, Jena, Germany) in the confocal mode.

### Live cell microscopy

For microscopy experiments, platelets were loaded with calcium fluorophores and immobilized by either incubation of platelet suspension in the flow chamber for 5 min or by perfusing whole blood over the surface at a shear rate of 200 s<sup>-1</sup> for 5 min. For TIRF microscopy, platelets were immobilized either on fucoidan (100  $\mu$ g/mL) or anti-CD31 (VM-64) (48) and investigated in flow chambers (52). An inverted Nikon Eclipse Ti-E microscope equipped with 100 $\times$ /1.49 NA TIRF oil objective was used. Cells were observed in DIC and TIRF modes. A 405-nm laser was applied to assess calcium-free Fura-2 fluorescence in a platelet. Calcium concentration was assessed from Fura-2 fluorescence as a ratio of initial/running values, taking exponential bleaching of the dye into account. For temperature fixation, during observation, a lens heater (Biophtechs, Butler, PA) was used.

### Data analysis

Nikon NIS-Elements software was used for microscope image acquisition; ImageJ (<http://imagej.net/ImageJ>) was used for image processing for both

TIRF microscopy and Western blotting and microscopy assays from literature (21,38). For the CLEC-2 cluster size calculation, data were acquired directly from the figures from (38) without additional calibration. The absolute size of CLEC-2 clusters (Fig. S1 D) was calculated from the DyLight 594 FcPodoplanin fluorescence intensity (Fig. 5 A; (38)), which was assumed to be proportional to the number of receptors per cluster. It has also been assumed that only CLEC-2 monomers and dimers are present on the surface of resting platelets. Flow cytometry data were processed using FlowJo (<http://www.flowjo.com/>) software. Statistical analysis was performed in Python 3.6.

## Model solution and sensitivity analysis

The model, formed of ordinary differential equations (see Supporting Results) with initial variable values (Tables S2, S5, and S7), was integrated using the LSODA method in COPASI software. The stochastic model was solved using stochastic integration methods (combined Adaptive SSA/the  $\tau$ -leap method (46,53)) implemented in COPASI software, similar to previously published methods (45,54). Parameter estimation was performed using the Genetic Algorithm. Models are given in the Table S9.

Sensitivity score was calculated as  $Score = (O_a - O_i)/O_a$ , where  $O_i$  and  $O_a$  represent the model output (e.g., the steady state and time to reach the peak in Syk activity) in respect to the initial parameter set (obtained from parameter fitting) and the adapted parameter, respectively.

## RESULTS

### Scheme of biochemical reactions underlying our model of CLEC-2-induced platelet activation

The model development was carried out based on the known details of the CLEC-2 signaling network. Briefly, after the binding of CLEC-2 to its ligand, CLEC-2 receptor-ligand complexes rapidly form tight clusters, predominantly in the lipid rafts (35,36). Activated and clustered CLEC-2 molecules can be phosphorylated by platelet Syk tyrosine kinases (55). Although it has been proposed that Src family

kinases (SFKs) also participate in the process of CLEC-2 phosphorylation (56,57), here in the model, we considered SFKs merely as a positive mediator for Syk basal activation (17). The inactive Syk rapidly bound two phosphorylated CLEC-2 receptors by two Src homology 2 (SH-2) domains. Association with CLEC-2 resulted in Syk activation and stabilization of CLEC-2 dimers (17,58,59). Binding of SFKs to phosphorylated hemITAM also led to the complete SFK activation, which additionally amplified Syk activation (17,58). Syk activated T cell ubiquitin ligand-2 (TULA-2), which is a negative regulator Syk activation (44). Active Syk and SFKs phosphorylated an adaptor molecule called LAT, leading to LAT signalosome formation (34,40,60), which consists of PLC $\gamma$ 2, phosphoinositide-3-kinase (PI3K), SH2-domain-containing leukocyte phosphoprotein of 76 kDa (SLP-76), and a set of other adaptor proteins. In the LAT signalosome, the PI3K became active and produced phosphoinositol-3,4,5 trisphosphate (PIP<sub>3</sub>) from phosphoinositol-4,5 bisphosphate (PIP<sub>2</sub>) in the surrounding plasma membrane region. The increase in PIP<sub>3</sub> concentration resulted in Bruton's tyrosine kinase (Btk) attraction to the region and phosphorylation and activation of PLC $\gamma$ 2 (61). Finally, PLC $\gamma$ 2 hydrolyzed PIP<sub>2</sub> and produced inositol-1,4,5 trisphosphate (IP<sub>3</sub>). IP<sub>3</sub> induced Ca<sup>2+</sup> signaling. A brief scheme of platelet CLEC-2 signaling (Fig. 1) described above was the basis of the constructed computational model.

### Computational model construction

The computational model of CLEC-2-induced platelet activation was designed according to the scheme above. It consisted of five compartments: extracellular space, plasma

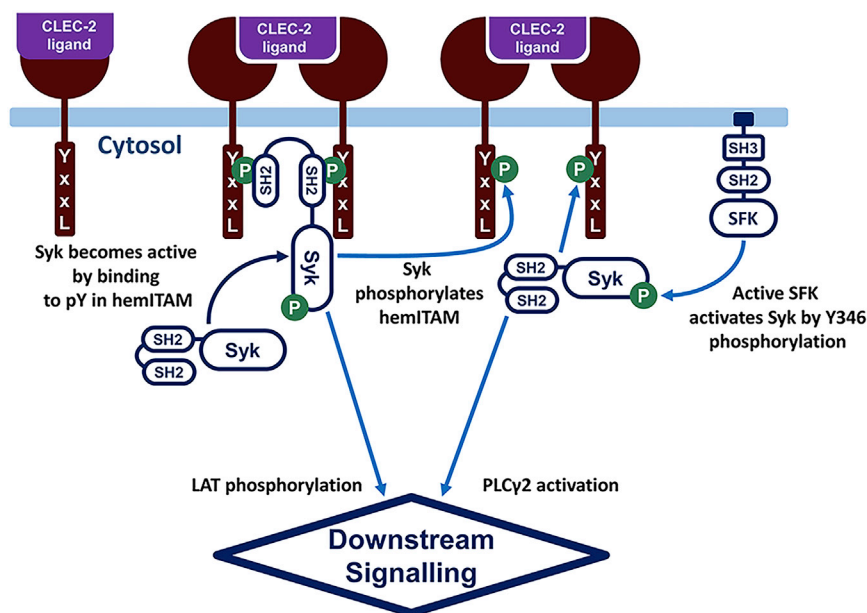


FIGURE 1 CLEC-2-induced signaling in blood platelets. In resting platelets, relatively few Syk kinases are active because of the low SFK activity. Upon ligation of the platelet CLEC-2 and CLEC-2 cluster formation, tyrosine residues in the CLEC-2 cytoplasmic domain (YxxL sequence, hemITAM) become phosphorylated by Syk kinases. Nonactive Syk kinases bind to phosphorylated hemITAM with its SH2 domains and become active via *trans*-autophosphorylation. Accumulation of the active Syk results in downstream platelet activation and calcium signaling. To see this figure in color, go online.



membrane, cytosol, dense tubular system (DTS) membrane, and DTS (Table S1). The model included the following biochemical modules: the “CLEC-2 clustering” module, capturing CLEC-2 ligand binding and cluster formation (Fig. 2 A; Tables S2–S4); the “quiescent state” module, capturing CD148 and C-terminal Src kinase (Csk)-mediated SFK activation and Syk primary activation by active SFKs (Fig. 2 B; Tables S5 and S6); the “tyrosine kinase” module, capturing CLEC-2 phosphorylation and activation of Syk and SFK kinases (Fig. 2 C; Tables S5 and S6); the “LAT-PLC $\gamma$ 2” module, capturing events downstream of activated Syk and SFKs, including phosphorylation of LAT, PI3K and

Btk incorporation to the signalosome, PLC $\gamma$ 2 activation, and production of IP $_3$  (Fig. 2 D; Tables S7 and S8); and the “calcium” module, capturing IP $_3$ -induced calcium signaling in platelet cytosol (from Fig. 2 D; (45,62)). The underlying systems of differential equations were constructed from current biological knowledge (see above) using the assumptions of either mass action or Henry-Michaelis-Menten kinetics. The probabilities in the corresponding stochastic model were calculated based on the same assumptions. The parameter values were taken from the experimental reports on the corresponding human enzymes, whereas the numbers of proteins per platelet were

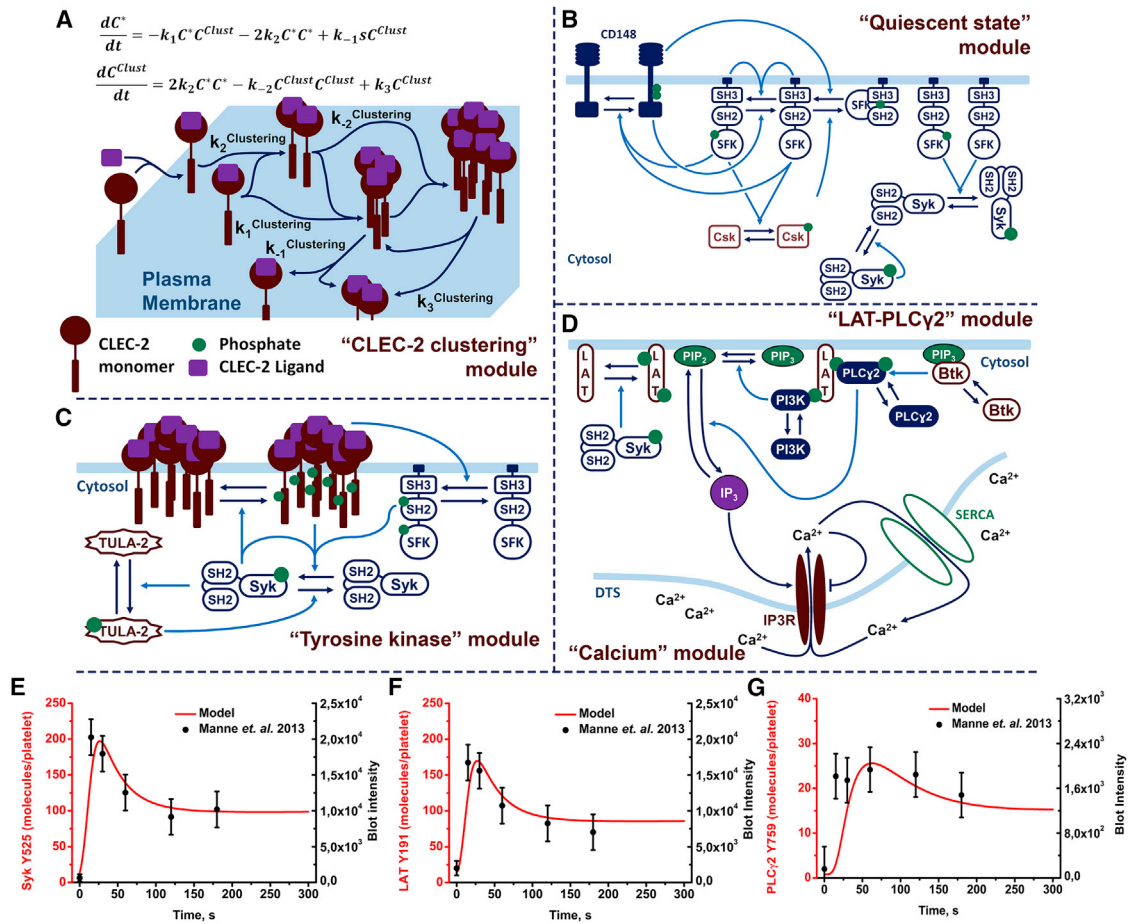


FIGURE 2 Scheme of the model of platelet CLEC-2 signaling. The “CLEC-2 clustering” module (A) after CLEC-2 ligation CLEC-2 molecules to formed clusters is shown here. The model of the CLEC-2 clustering is based on Filkova et al. (64). Activated CLEC-2 molecules could form CLEC-2 clusters, which could form larger clusters by binding single-activated CLEC-2 molecules or other clusters. The clusters decayed into cluster and cluster or cluster and single-CLEC-2 molecule. The “quiescent state” module (B) shows that active CD148 produces one-third-active SFKs, which are negatively regulated by active Csk. One-third-active SFKs autophosphorylated and became two-thirds-active SFKs. Active CD148 negatively regulated this reaction. All forms of active SFKs mediated CD148, Csk, and Syk activation. Active Syk activated nonactive Syk. The “tyrosine kinase” module (C) shows that after cluster formation, active Syk phosphorylated hemITAM in the CLEC-2 cytoplasmic domains. Inactive Syk or two-thirds-active SFKs bound phospho-hemITAMs (two for Syk and one for SFKs) with their SH2 domains and became active. Active Syk also mediated TULA-2 phosphatase activation, which is a negative regulator of Syk activity. “LAT-PLC $\gamma$ 2” module (D) shows that active Syk phosphorylated the adaptor protein LAT. PLC $\gamma$ 2 and PI3K bound P-LAT, which activated PI3K. Active PI3K phosphorylated PIP $_2$  and produced PIP $_3$ , which became a docking site for Btk. Btk activated upon PIP $_3$  binding and activated PLC $\gamma$ 2. Active PLC $\gamma$ 2 hydrolyzed PIP $_2$  and produced IP $_3$ . The “calcium” module (D) shows that IP $_3$  activated IP $_3$ R on the surface of the DTS. Through active IP $_3$ R, free Ca $^{2+}$  ions passed to the cytosol. Ca $^{2+}$  inhibited IP $_3$ R as well and returned to the DTS via SERCA. Dark blue lines represented transitions between species; light blue lines represented catalysis. Copy numbers of active Syk (E), LAT (F), and PLC $\gamma$ 2 (G) were fitted to experimental data on fucoidan-induced platelet activation from Manne et al. (21), error bars represent 10% from the experimental values. To see this figure in color, go online.

taken from the published proteomics data (63). The model reactions, equations, and parameter values can be found in [Supporting Results](#).

The “CLEC-2 clustering” module described the process of receptor clustering. Mathematically, this description was performed by two differential equations, based on our previously published study (64). This approach was called the “two-equation” model (Fig. 2 A). Its applicability and correspondence to an explicit model of receptor cluster formation (called the “N-equation” model) and experimental data are given in the Fig. S1. The “two-equation” model described the behavior of variables for the concentration of single CLEC-2 molecules and the concentration of CLEC-2 clusters in the plasma membrane (Fig. 2 A; Fig. S1 B). During the estimation of the “CLEC-2 clustering” module parameters, we identified two distinct patterns of receptor clustering in the “two-equation” model. The first, which could be called “ligand-mediated” cluster formation, suggested that the clustering coincides with receptor ligation. The second, called the “postligation” cluster formation, suggested that the clusters appear after the formation of receptor-ligand complexes. Both patterns will be discussed further in [Two Different Clustering Patterns Predicted by the Model](#). All of the model calculations were performed with “ligand-mediated” cluster formation model, except where otherwise stated.

For the “quiescent state” module, the unknown parameters were tuned to obtain 5% of active Syk kinases and 10% of active SFK kinases at the steady state achieved without CLEC-2 ligand in the system. The CD148 phosphatase and Csk kinase were introduced into the model to maintain this steady state (Fig. 2 B). For the “tyrosine kinase” module, we assumed that the first event was the phosphorylation of CLEC-2 in clusters by Syk kinases. The activation of Syk kinases, as well as SFK activation, was assumed to occur depending on the CLEC-2 cluster size. The descriptions of the “LAT-PLC $\gamma$ 2” module and the “calcium” module can be found in the [Supporting Results](#) (Fig. 2 D). It is noteworthy that the only link between the “calcium” module and the other modules was the IP $_3$  concentration, which, in its turn, was mediated by active PLC $\gamma$ 2. That is why we chose the number of active PLC $\gamma$ 2 as one of the major model output. A network diagram depicting all of the reactions and parameters of the model is given in Fig. S2. The corresponding Systems Biology Markup Language files can be found in [Data S1](#) (also see [Table S9](#) for details).

The full model was constructed as a sum of the separate models described above without further adjustment of the parameters. The full model appeared to be capable of the correct description of the following experimental data. The predicted numbers of active Syk, SFKs, and the phosphorylated LAT (Fig. 2, E and F, and Fig. S3, respectively) were in good agreement with available information from experimental literature data (21). However, the predicted numbers of active PLC $\gamma$ 2 described the data less accurately

(Fig. 2 G), which could be caused by the secondary activation of platelets under the conditions of the experiment.

## Two different clustering patterns predicted by the model

In the process of parameter estimation for the “CLEC-2 clustering” module, we identified two different possible sets of parameters from which the model could describe experimental data Pollitt et al. (Figs. 3 and S1 D; (38)). The first observed pattern was called a “ligand-mediated” receptor clustering when the rapid receptor dimerization immediately followed the receptors’ ligation (Fig. 3 A). The “ligand-mediated” receptor-clustering mode corresponds to the ligand-driven receptor-clustering mechanism in vivo. The second pattern, when the receptors’ ligation did not directly lead to receptor dimerization, was termed “postligation” (Fig. 3 A). This mode corresponded to the assumption that CLEC-2 receptor undergoes additional conformational changes after ligation, which made it more prone to clustering. The comparison of the average cluster size between two different schemes is given in Fig. 3 B. Parameter variation results revealed that the maximal size of the CLEC-2 clusters is determined by the total number of CLEC-2 as well as kinetic parameters of the clustering, for both the “ligand-mediated” (Fig. S4, A–C) and “postligation” (Fig. S4, G–L) clustering regimes. However, in the “ligand-mediated” clustering regime, the maximal CLEC-2 cluster size appeared to be more sensitive to the assessed parameters than in the “postligation” regime (Fig. S4).

With both schemes, the full model predicted cytosolic calcium spiking (Fig. 3 A). However, the “postligation” scheme could not be tuned to induce calcium spiking earlier than 200 s after ligand introduction (Fig. 3, A and D), despite producing a more significant increase in the number of active PLC $\gamma$ 2 (Fig. 3 C) and higher concentration of cytosolic calcium in the cell population (Fig. 3 D). However, previous experimental data (21) suggested much shorter activation times for CLEC-2-induced platelet activation, and thus, we preferred the “ligation-mediated” scheme. Curiously, a rapid dimerization of ITAM receptors was demonstrated to correlate with the shortened cell activation lag-times elsewhere (41).

## Sensitivity analysis of the model

To analyze the influence of unknown parameters and determine the possible rate-limiting steps, we performed a local sensitivity analysis (Fig. 4; Figs. S5–S16). Scaled local sensitivities of the time to reach the peak quantities/concentrations of active Syk ( $S^*$ ), phosphorylated LAT ( $L^*$ ), active PLC $\gamma$ 2 ( $p^*$ ), IP $_3$  ( $I_3$ ), and cytosolic Ca $^{2+}$  to all model parameter values were calculated. The results are given in Figs. 4 A and S5. Parameters of the “tyrosine kinase” module had the biggest impact on all of the analyzed variables. The “LAT-PLC $\gamma$ 2” module parameters were less influential, and the “CLEC-2

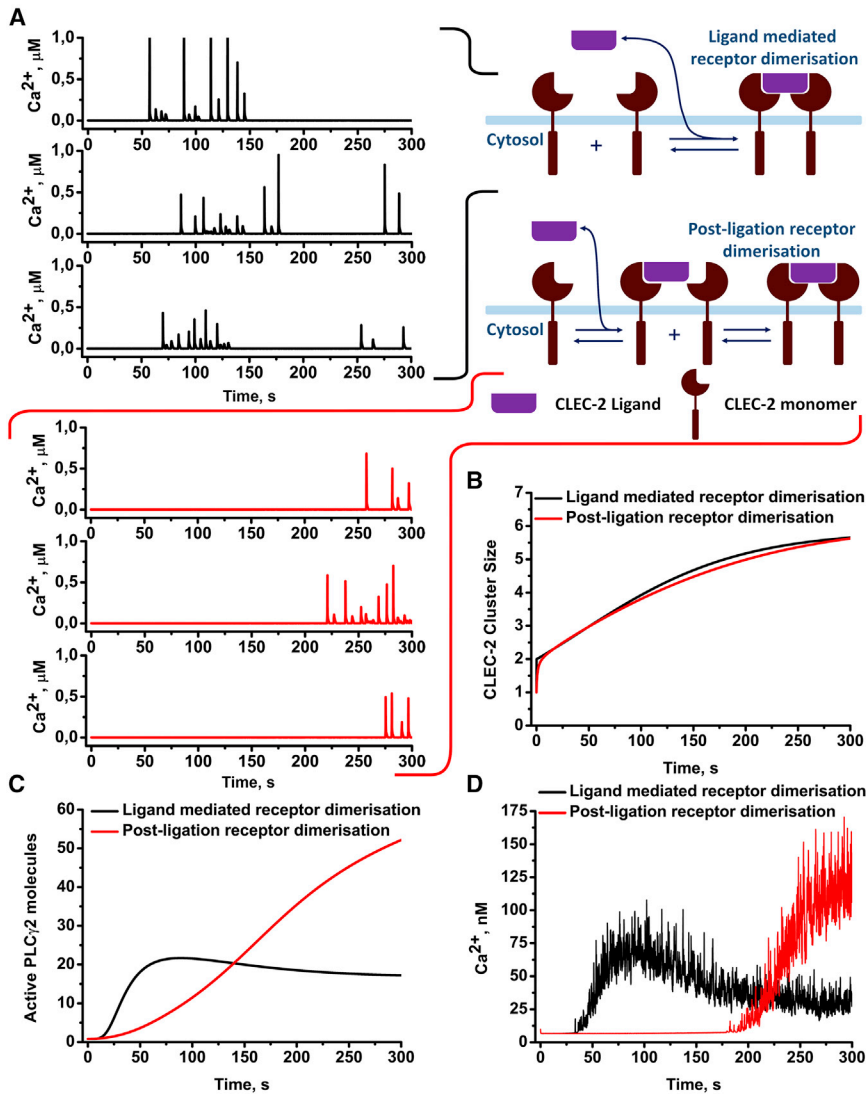


FIGURE 3 Comparison of the receptor-clustering patterns effects on platelet CLEC-2-induced activation. Two patterns of receptor clustering are shown: ligand-mediated receptor clustering (rapid receptor dimerization upon ligation, *black*) and postligation clustering (ligation does not lead to rapid receptor dimerization, *red*). (A) Both approaches resulted in cytosolic calcium spiking. However, the postligation model resulted in a significantly delayed activation in comparison with the rapid-dimerization model (B and C). Averaging of the calcium concentration over 500 stochastic runs of the model also demonstrated that the delayed model demonstrated a significantly delayed but yet amplified response in comparison to the rapid-dimerization model (D). To see this figure in color, go online.

clustering” module parameters were the least influential. The “tyrosine kinase” module parameters concerning Syk ( $[Syk]_0$ ,  $k_{cat}^{Syk}$ ,  $Km^{Syk}$ , and  $k_{S1}^{SH2}$ ) influenced all platelet responses, whereas its parameter for CLEC-2 dephosphorylation rate ( $Kr^{Phosph}$ ) was the most influential only for  $S^*$  (active Syk). Among the “LAT-PLC $\gamma$ 2” module parameters, the most influential parameters were the reverse rate of LAT phosphorylation and LAT concentration ( $Kr^{LAT}$ ,  $[LAT]_0$  for all of the variables, except Syk) and the catalytic parameters of Btk kinase ( $k_{cat}^{Btk}$ ,  $Km^{Btk}$ , for all variables except Btk). Finally, among parameters of the “CLEC-2 clustering” module,  $k_{-2}$ ,  $k_{-1}$ , and  $k_1$ , along with CLEC-2 initial concentration, were influential for all responses. Explicit variation of the most influential model parameters for PLC $\gamma$ 2 is given in Fig. 4, B–M. Variation of the rest of parameters concerning all of the analyzed variables and sensitivity scores for all of the variables can be found in Figs. S6–S16 and Tables S10–S14, correspondingly. Based on these results, we can conclude that the most influential pa-

rameters for all of the analyzed variables concern Syk kinase activation ( $k_{S1}^{SH2}$ ,  $k_{cat}^{Syk}$ ,  $Km^{Syk}$ ). On the other hand, parameters, governing reverse reactions ( $Kr^{Phosph}$ ,  $Kr^{LAT}$ ,  $Kr^{Syk}$ ), as well as parameters concerning TULA-2 activation ( $Kf_{Syk}^{TULA2}$ ,  $Kr_{Syk}^{TULA2}$ ,  $Kf_{TULA2}^{Syk}$ ), also were among the most influential, which highlights the role of the negative regulators of signaling for CLEC-2-induced platelet activation. Finally, local sensitivity analysis also allowed the identification of three rate-limiting reactions: Syk kinase activation, LAT phosphorylation, and CLEC-2 cluster formation. Among these reactions, Syk activation was the most influential.

### CLEC-2 agonist fucoidan is capable of evoking calcium response in platelets independently from secondary mediators of signaling

One of the model predictions suggested that CLEC-2 stimulation was sufficient to initiate calcium signaling in

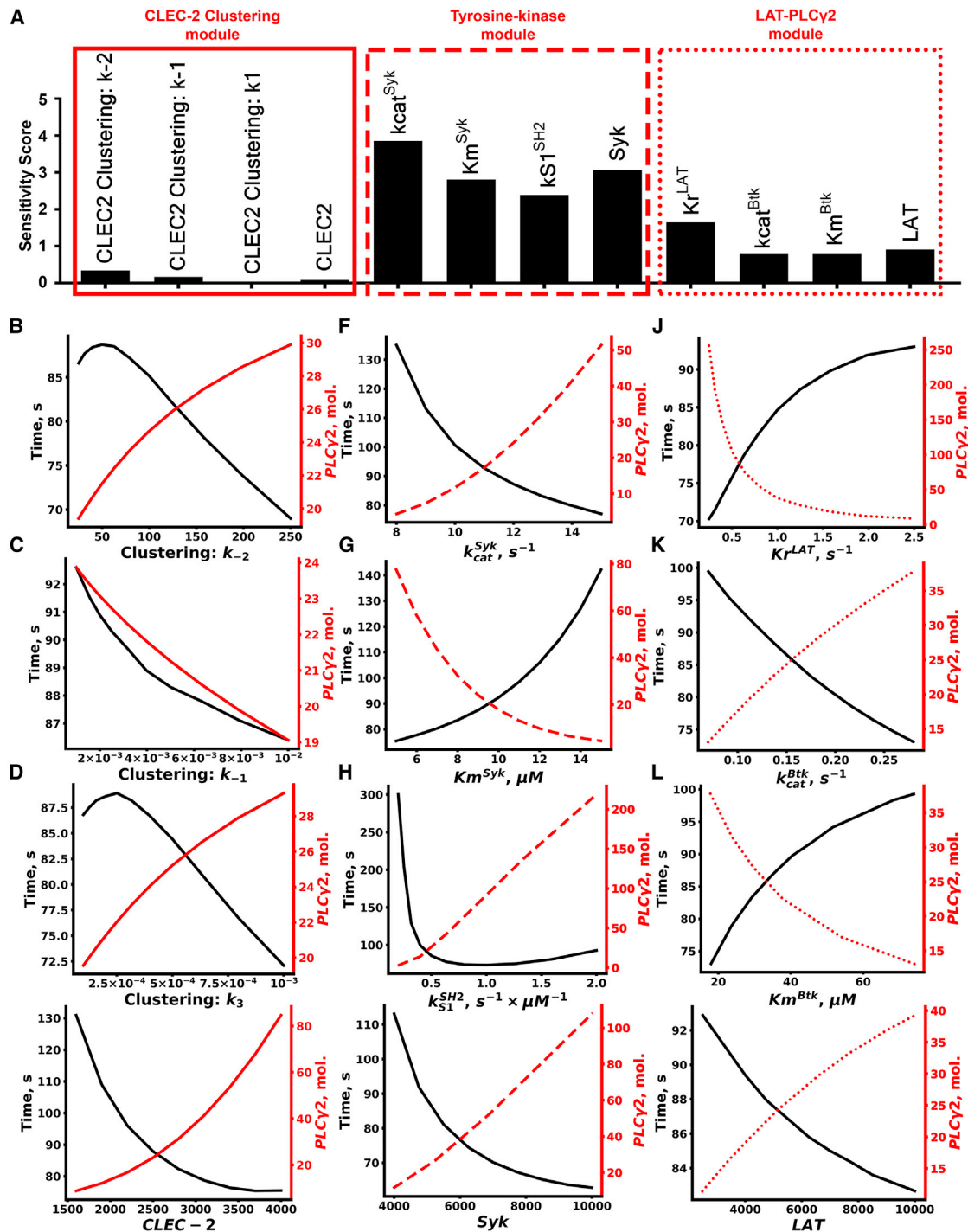


FIGURE 4 Sensitivity analysis and variation of the unknown parameters. Sensitivity scores for the effect of parameter variation on the concentration of active PLC $\gamma$ 2 were calculated (A). Explicit variation of the parameters with the highest sensitivity scores for the effect on maximal PLC $\gamma$ 2 number and time to reach the maximum for CLEC-2 clustering  $k_{-2}$  (B), CLEC-2 clustering  $k_{-1}$  (C), CLEC-2 clustering  $k_3$  (D), CLEC-2 initial number (E), turnover rate of Syk kinases (F), Michaelis constant of Syk kinases (G), forward rate of Syk activation upon SH-2 domain binding to dually phosphorylated hemITAMs (H), Syk initial number (I), reverse rate of LAT phosphorylation (J), turnover rate of Btk (K), Michaelis constant of Btk (L), and LAT initial number (M) are shown. To see this figure in color, go online.

platelets (Fig. 3, A and D). To test this prediction, we performed flow cytometry experiments on platelets loaded with calcium fluorophore Fura Red (Fig. 5 A). To avoid an

impact from secondary activation, we preincubated platelets with P2Y1 receptor antagonist MRS2179 (Fig. 5 A). To assess the predicted dependence of platelet activation on



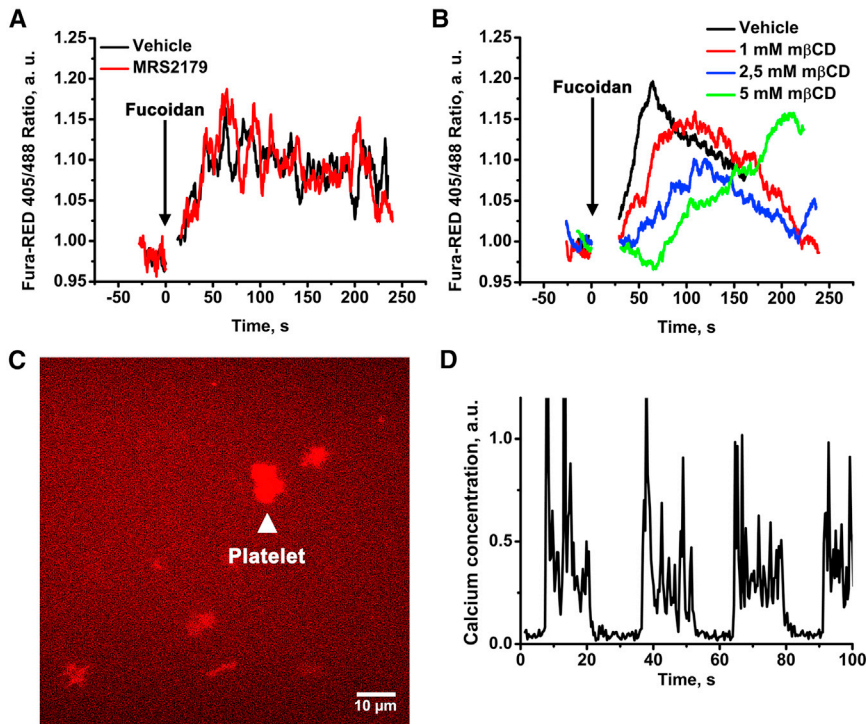


FIGURE 5 CLEC-2-evoked calcium signaling in platelets. Continuous flow cytometry analysis of highly diluted platelet suspension ( $1 \times 10^3$  plt/mL) revealed that CLEC-2 agonist fucoidan-induced calcium response is independent of the presence of MRS2179 (A) while being gradually dependent on the concentration of  $m\beta$ CD (B). Single-cell analysis using TIRF microscopy revealed that platelets are capable of spreading on fucoidan-covered glass (C) and that immobilized fucoidan is capable of evoking calcium oscillations in platelets (D). To see this figure in color, go online.

the clustering of CLEC-2, we investigated the influence of membrane cholesterol content on calcium response. Cholesterol molecules determine the stability of membrane regions, and thus, incubation of cells with a cholesterol-binding agent  $m\beta$ CD could disrupt clusters of proteins (51). During experiments, we observed that although high concentrations (5 mM) of  $m\beta$ CD were capable of severe disruption of platelet response to fucoidan (Fig. 5 B), relatively low concentrations of  $m\beta$ CD (1 mM) delayed platelet activation without affecting its degree (Fig. 5 B). This observation was in agreement with model predictions (Fig. 3 D), supporting rapid clustering pattern for CLEC-2 (Fig. 3 A). To test the prediction of the model that fucoidan induces rare calcium spiking in platelets instead of a stationary increase in calcium concentration (Fig. 3 A), we performed analysis of single-cell calcium signaling using fluorescence microscopy (Fig. 5, C and D). Washed Fura-Red-loaded platelets spread on fucoidan-covered glass (Fig. 5 C), which resulted in prolonged calcium spiking (Fig. 5 D). This observation supported the model prediction that fucoidan is capable of calcium spiking induction.

#### Impact of the medium temperature and plasma membrane fluidity on CLEC-2 induced calcium response in platelet suspension

We have performed further investigation of fucoidan-induced intracellular signaling in platelets in the presence of  $m\beta$ CD and temperature variation to test the model predic-

tions on the role of the receptor-clustering process. At both room (25°C) and body (37°C) temperature, activation of platelets with fucoidan led to an increase in cytosolic  $Ca^{2+}$  concentration (Fig. 6 A). However, at 25°C, this increase occurred at 100 s, whereas at 37°C, it was significantly more rapid and occurred at 60 s. Preincubation of platelets with  $m\beta$ CD further delayed the increase in the concentration of cytosolic calcium both at 25°C (240 s) and at 37°C (105 s) (Fig. 6 B). It should be noted that temperature variation did not affect the activation of platelets by low concentrations (2  $\mu$ M) of ADP (Fig. S17).

Single-cell analysis by means of immunofluorescent microscopy revealed that at 37°C, clustered fractions of phosphorylated LAT, which are known markers of cholesterol-enriched microdomains in the platelet membrane (34), appeared at 30 s, and the amount of phosphorylated LAT reached its maximal values by 60 s (Fig. 6 C; Fig. S18). It is noteworthy that at most time points, the bright phosphorylated LAT (LATp) fluorescence spots could be observed. The lower medium temperature and cholesterol depletion by 1 mM  $m\beta$ CD resulted in delayed LATp phosphorylation and decreased clustering (Figs. S19 and S20, correspondingly). Platelets activated by C-reactive protein exhibited the most significant increase in LATp phosphorylation after 300 s (Fig. S21). The “CLEC-2 clustering” module parameter variation ( $k_1$  and  $k_3$  decrease and  $k_2$  increase) allowed us to accurately describe the decrease in LAT phosphorylation upon temperature lowering and cholesterol depletion (Fig. 6 C; Table S15).

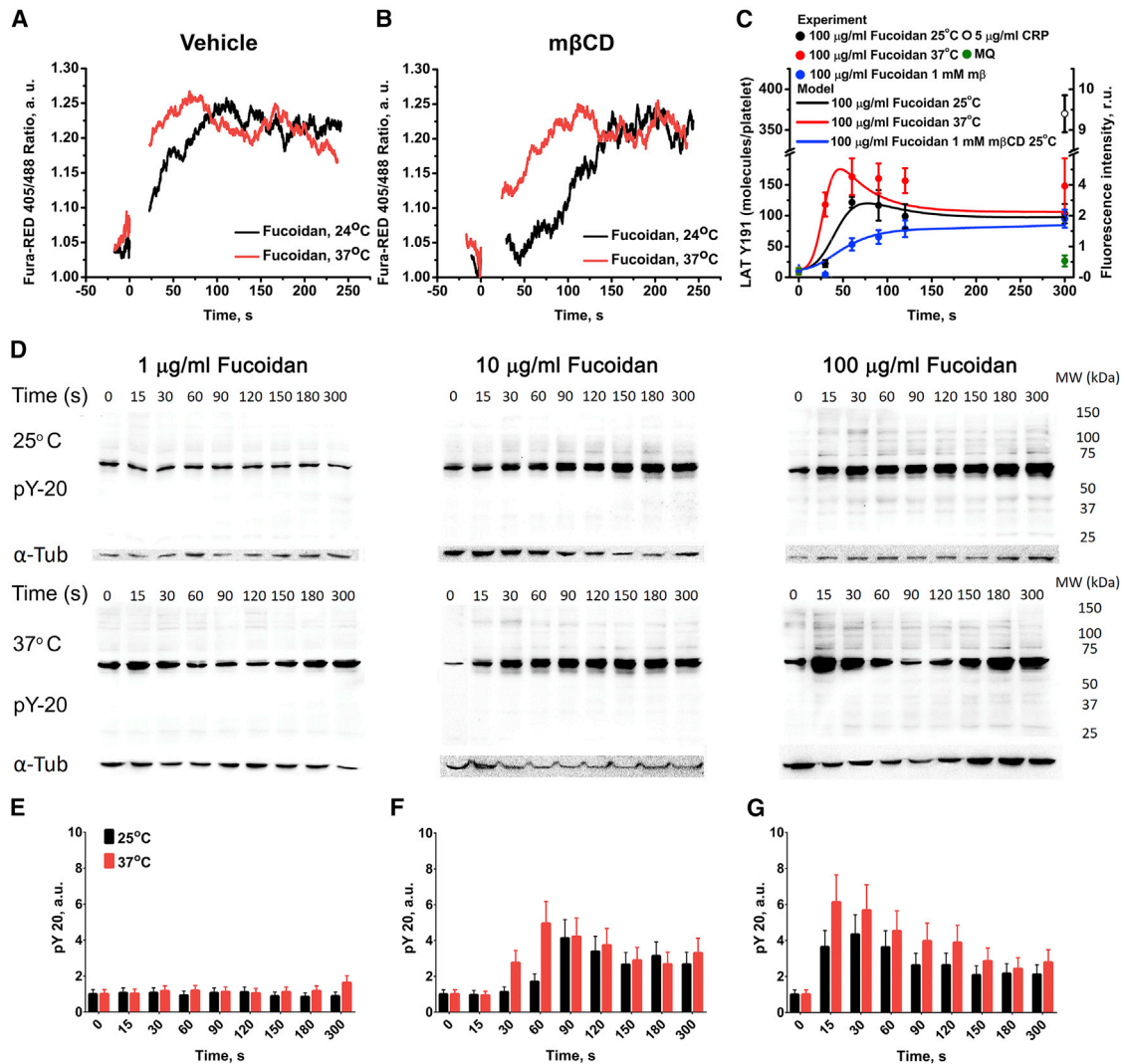


FIGURE 6 Platelet CLEC-2 signaling is dependent on temperature conditions. Flow cytometry assay of CLEC-2 induced signaling in platelets after activation by 100  $\mu\text{g}/\text{mL}$  of fucoidan. Activation at 25°C was significantly slower than at 37°C (A). Disruption of lipid rafts by  $m\beta\text{CD}$  delayed activation (B). Each curve represents data from at least three experiments. (C) Comparison of the immunofluorescent assays with computational model predictions describing the dependence of platelet CLEC-2-induced activation from medium temperature and cholesterol presence in the cell membrane. Each experimental time point is averaged over 50 platelets. Error bars represent SEM. (D–G) Immunoblot assay of CLEC-2-induced signaling is shown (D shows raw data); platelets were activated by 1 (E), 10 (F), and 100 (G)  $\mu\text{g}/\text{mL}$  of fucoidan at 25 or 37°C. Samples for analysis were taken 0, 15, 30, 60, 90, 120, 150, 180, and 300 s after activation. Murine anti-human-phosphotyrosine primary antibodies (PY-20 clone) were used. Anti-tubulin primary antibodies were used as loading control after stripping. A typical experiment is shown for one out of  $n = 3$  different donors, error bars represent SD. To see this figure in color, go online.

To investigate which part of the CLEC-2 signaling cascade is influenced by the temperature changes, we performed immunoblotting analysis of tyrosine phosphorylation level in platelets activated by fucoidan at room and body temperature (Fig. 6, D–G). Washed human platelets at a concentration of  $1.5 \times 10^9/\text{mL}$  in modified Tyrode's buffer (no BSA and no  $\text{Ca}^{2+}$ ) were incubated with fucoidan for 0–5 min at given temperature conditions. Samples were taken at 15- to 30-s time intervals and analyzed by immunoblotting with anti-phosphotyrosine antibody PY20, as described in Methods. The analysis shows that 1  $\mu\text{g}/\text{mL}$  of fucoidan does not induce significant activation. On the other hand, both 10 and 100  $\mu\text{g}/\text{mL}$  of fucoidan induced tyrosine phosphorylation with peak values at 90

and 30 s, respectively. The increase in temperature significantly shortened the lag-times of phosphorylation to 60 and 15 s, respectively. Thus, we can conclude that the temperature variation influences the activity of tyrosine kinases as well as calcium signaling. This result is in agreement with the model prediction that the rate of CLEC-2 clustering determines the time-lapse to peak platelet activation.

### Impact of the medium temperature on CLEC-2 induced calcium response in single cells

TIRF microscopy of immobilized single-calcium-sensitive-dye-loaded platelets was performed to investigate the nature

of the cytosolic calcium increase observed in flow cytometry. We utilized two experimental settings. In the first setting, platelets were immobilized on VM64 (anti-CD31 clone (48)) antibody (Fig. 7, A–D), and the fucoidan solution in Tyrode’s buffer was washed over the surface. Platelets developed cytosolic calcium spiking with varying intensities (Fig. 7, A and C). Frequent cytosolic calcium spiking intensified by 50 s after fucoidan addition (Fig. 7, A–D). Maximal calcium concentration in the spikes as well as spike frequency corresponded with the model predictions (Fig. 5 A). Comparison between fucoidan-induced calcium spiking between 25 (Fig. 7 A) and 37°C (Fig. 7 C) shows that the frequency of spiking increases at body temperature, and there is also a noticeable increase in amplitude. This result corresponds to the prediction that fucoidan-induced platelet activation could be influenced by the temperature-dependent parameters: receptor translocation and enzyme turnover rates. Together, these data corroborate the model predictions that 1) fucoidan induces calcium spiking in platelets and 2) fucoidan-induced activation of platelets is significantly influenced by temperature. It could be noticed that although the amplitudes of the calcium spikes remained around the same values at different temperatures (Fig. 7 F), the interspike time intervals were significantly shorter at 37°C than at 25°C (Fig. 7 E). This observation corresponded with the model prediction that an increase in CLEC-2 clustering rates in the membrane lead to an increase in cytosolic calcium spiking (Fig. S22).

## DISCUSSION

Here, we aimed at investigation of primary regulatory mechanisms of platelet CLEC-2-induced activation by means of comprehensive computational systems biology modeling. Our model accurately reproduced literature data on platelet activation by CLEC-2 agonists fucoidan, rhodocytin, and podoplanin. The model gave a set of predictions. First, a rapid CLEC-2 clustering upon ligation was required for platelet activation by CLEC-2 agonists, which corresponded to data from Mukherjee et al. (41) and our experiments with m $\beta$ CD-treated platelets (Fig. 5 B). Second, CLEC-2 ligands are capable of inducing cytosolic calcium spiking independent of platelet secondary activation, which corresponded to data from Badolia et al. (40) and our experiments with MRS2179 (Figs. 5 A and 6, A and B). Third, the sensitivity analysis of the model has revealed a key role of Syk kinases in the CLEC-2 signaling cascade (Fig. 3), which was in perfect agreement with Hughes et al. (17) and Séverin et al.

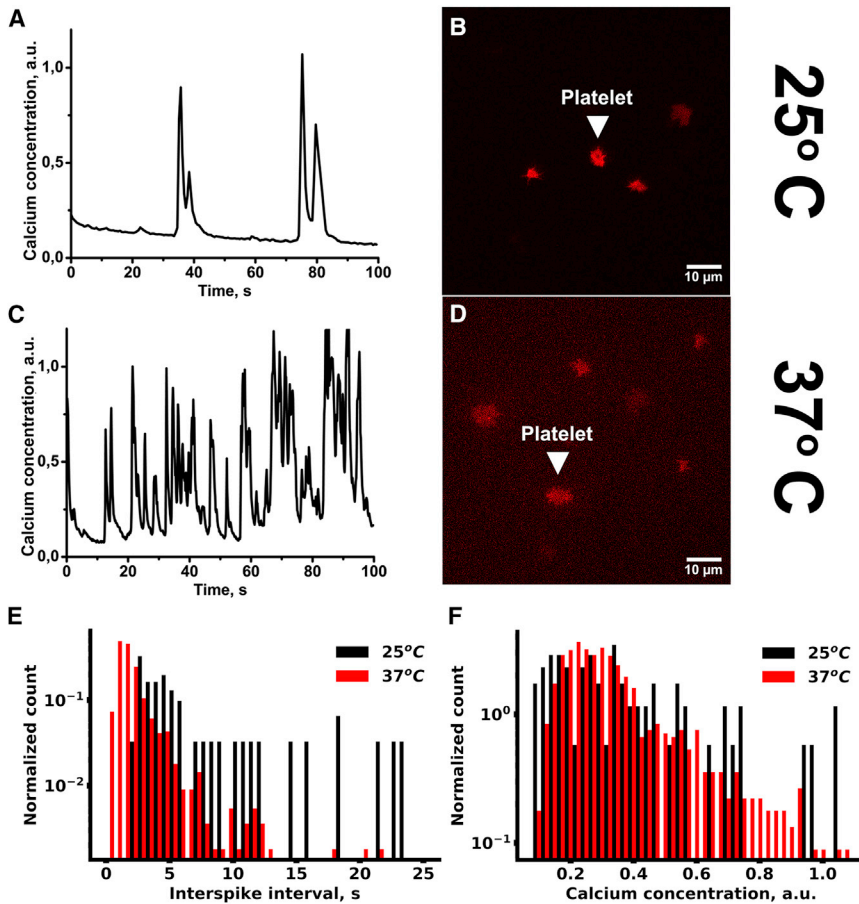


FIGURE 7 Cytosolic calcium spiking induced by fucoidan in single cells. Platelets were loaded with Fura-2, immobilized on VM-64 (A–D), and then illuminated by 405-nm laser. Cytosolic calcium concentration was recalculated from Fura-2 fluorescence (see Methods). Washed platelets were immobilized on the VM64 antibody (A–D). At time point “0,” the fucoidan solution at 100  $\mu$ g/mL was added. Cytosolic calcium spiking (A and C) and whole-cell fluorescence (B and D) were monitored at room temperature (A and B) or 37°C (C and D). Representative curves are shown out of  $n = 10$ . (E and F) Intervals between calcium spikes (E) and calcium concentration per spike (F), spread on VM-64 and activated by fucoidan at 25°C (black) or 37°C (red), are shown. Data were collected from 20 cells. To see this figure in color, go online.

(55). Finally, the CLEC-2 clustering and LAT signalosome formation appeared to be the rate-limiting steps in signal propagation in addition to tyrosine kinase activities. This proposition was supported by our experiments at different temperature conditions alongside different  $m\beta$ CD concentrations (Figs. 6 and 7).

During model development, we applied mathematical equations from our previously published model of platelet aggregation (64) to describe the process of receptor clustering (“two-equation” model, Fig. S1 B). The “two-equation” model described experimental data on CLEC-2 receptor clustering, as well as the computational results of a more conventional model of receptor clustering (“*N*-equation” model, Fig. S1 A). Two possible receptor-clustering patterns distinctive in the sequence of dimerization and ligation of receptors were identified. However, only the inclusion of the pattern with rapid dimerization in the model allowed it to reproduce an experimentally observed calcium response (Fig. 3, C and D). The “ligand-mediated receptor dimerization” clustering pattern was in line with experimental data describing the capability of the CLEC-2 ligand to promote receptor clustering (35–37). Furthermore, this result was in agreement with previously published data on other ITAM-bearing receptors (41). On the other hand, CLEC-2 clustering upon activation by monomeric ligands (e.g., podoplanin) has been reported (38), which should correspond to “postligation” clustering, assuming conformational changes in the CLEC-2 structure upon ligation.

The analysis of the model predicted a central role of the Syk tyrosine kinase for CLEC-2 signaling cascade (Fig. 4 A). This prediction corresponded to previously published data on CLEC-2 stimulation in platelets pretreated with PRT-060318 (56), as well as CLEC-2 stimulation of platelets of mice deficient in Syk-activating SH-2 domains (17). Sensitivity analysis has also revealed that, in addition to the tyrosine kinase activity, the PLC $\gamma$ 2 activity and receptor clustering, to a lesser extent, are the rate-limiting steps as well (Fig. 4). It is noteworthy that the parameters concerning dephosphorylation of signaling were as influential as the parameters concerning the activation of kinases (Fig. 4; Fig. S5). This result emphasizes the role of the negative regulators of intracellular signaling for CLEC-2-induced platelet activation.

More accurate analysis of the parts of the platelet response influenced by the parameters revealed that, although the activity of tyrosine kinases had the most impact on every response, only CLEC-2 clustering influenced the time-lapse to peak concentration while only moderately affecting the number of active signaling proteins. This observation was supported by the decrease in platelet activation time with temperature increase or  $m\beta$ CD supplementation (Fig. 6, A and B). A similar effect could be expected from GPVI signaling, which also requires clustering of receptors. Indeed, when GPVI cluster formation was

affected by losartan, a delay in platelet response to collagen appeared (65).

To test the model predictions that CLEC-2 clustering is one of the rate-limiting processes for the CLEC-2 signaling cascade, we investigated the influence of two membrane-fluidity-changing agents on platelet activation. First, we utilized incubation of platelets with a cholesterol-binding agent  $m\beta$ CD, which changes membrane cholesterol saturation, and thus directly increases the fluidity of the membranes. We observed a faster platelet response to CLEC-2 agonists in the presence of  $m\beta$ CD (Figs. 5 B and 6 B). However, these results were in disagreement with previously published work (60) in which CLEC-2 signaling was shown to be independent of lipid rafts, and the lipid raft role was proposed mainly for secondary signaling. On the other hand, in Manne et al. (60), platelets were incubated with  $m\beta$ CD for an hour, and this could have led to the reintroduction of cholesterol in the signaling region (51). The dose-dependent response to  $m\beta$ CD, obtained upon incubation for 15 min in our work (Fig. S3 B), proves the membrane fluidity to be of significance for primary CLEC-2 response.

The second way to influence the rate of CLEC-2 clustering utilized here was a variation in the environment temperature. The temperature decrease from 37 to 25°C resulted in a prolonged delay after activation (Figs. 6 and 7). This result could not be considered as a direct confirmation of the receptor-clustering impact because it is well known that the temperature affects the turnover numbers of enzymes (66,67) to the same degree as the rates of diffusion (68,69). Experimental data on immunofluorescence microscopy additionally demonstrated impairment of LAT signalosome formation upon temperature decrease and cholesterol depletion (Fig. 6 C; Figs. S18–S20). Based on the model predictions, this is justified by the alterations in the receptor cluster formation at different conditions (Fig. 6 C). Furthermore, the fact that the applied decrease in temperature did not affect the degree of activation is in agreement with the model prediction that the receptor clustering affects only the times of activation, whereas tyrosine kinase activity controls both the time and the degree of activation (Fig. 4, B–E; Fig. S8). Additionally, we demonstrated that such a temperature variation has no significant effect on ADP-induced platelet activation, confirming the hypothesis that receptor clustering is specifically important for tyrosine kinase signaling (Fig. S17).

Among the main features of the model was its capability to work both in stochastic and in deterministic modes. The applicability of stochastic modeling to platelets is based on the fact that even at maximal degrees of activation upon CLEC-2 stimulation, amounts of crucial signaling proteins do not exceed 200 (Syk, LAT, PLC $\gamma$ 2).

Although the experimental data supported our model predictions, some limitations should be noted. Although it has been shown that fucoidan is capable of activating platelet CLEC-2 (21), it has been demonstrated recently that



fucoidan might be activating GPVI and platelet endothelial aggregation receptor 1 (PEAR-1) as well (70,71). However, PEAR-1 and GPVI participation in fucoidan-induced platelet activation has been demonstrated by aggregometry (70), in which the effects of secondary mediators of signaling are prevailing (34). Authors of Kardeby et al. (70) also report that fucoidan is not inducing calcium signaling in platelets solely by implicating spectrofluorimetry, which is insensitive to weak calcium signaling.

The confirmations of model predictions here are limited to experiments with isolated platelets. A large part of the model predictions is concerned with kinase activity not routinely assessed for single cells. For the experiments with immunoblotting, the distinction between primary and secondary signaling for tyrosine phosphorylation assays is not evident. Additional experiments on the roles of tyrosine kinases in CLEC-2 signaling, as well as further model development (direct inclusion of the protein-tyrosine phosphatase 1B (PTP1B) phosphatase) and investigation of cooperativity between CLEC-2 and GPVI, should be the subject of further studies.

The fact that the motion of proteins drives CLEC-2 activation in the plasma membrane and the assembly of signaling complexes demonstrated here allows us to take a new perspective on all receptors that perform clustering after activation or are associated with specific lipid microdomains. The knowledge of the underlying mechanisms of receptor cluster assembly will push forward understanding of molecular signaling in all types of eukaryotic cells, as well as the development of new antithrombotic agents specifically targeting receptor cluster formation.

## SUPPORTING MATERIAL

Supporting Material can be found online at <https://doi.org/10.1016/j.bpj.2020.04.023>.

## AUTHOR CONTRIBUTIONS

A.A.M. developed the model, performed simulations, performed experiments (flow cytometry, immunoblotting, immunofluorescent microscopy), analyzed the data, and wrote the article. F.A.B. performed single-cell microscopy experiments. J.M.G. and J.L.D. analyzed the data and edited the article. M.A.P. supervised the project and edited the article. A.N.S. planned model development and research, analyzed the data, performed experiments (microscopy), and edited the article.

## ACKNOWLEDGMENTS

We thank Prof. F.I. Ataullakhanov (CTP PCP RAS, Moscow, RF), Dr. A.V. Mazurov (NMRC of Cardiology, Moscow, RF), and Dr. N.E. Ustuzhanina (Zelinsky Institute of Organic Chemistry RAS, Moscow, RF) for reagents used during preliminary experiments and valuable discussions. We are grateful to Dr. A.V. Pichugin (Federal Medical Biological Agency, Moscow, RF) for advice and Miss V.N. Kaneva for assistance during flow cytometry data collection. We are grateful to Dr. S.I. Obydennyi for the advice and support during confocal microscopy data collection.

The study was supported by the Russian Science Foundation grant 17-74-20045.

## REFERENCES

1. Versteeg, H. H., J. W. M. Heemskerk, ..., P. H. Reitsma. 2013. New fundamentals in hemostasis. *Physiol. Rev.* 93:327–358.
2. van der Meijden, P. E. J., and J. W. M. Heemskerk. 2019. Platelet biology and functions: new concepts and clinical perspectives. *Nat. Rev. Cardiol.* 16:166–179, Published online November 14, 2018.
3. Repsold, L., R. Pool, ..., A. M. Joubert. 2017. An overview of the role of platelets in angiogenesis, apoptosis and autophagy in chronic myeloid leukaemia. *Cancer Cell Int.* 17:89.
4. Nurden, A. T. 2007. Platelets and tissue remodeling: extending the role of the blood clotting system. *Endocrinology.* 148:3053–3055.
5. Gawaz, M., and S. Vogel. 2013. Platelets in tissue repair: control of apoptosis and interactions with regenerative cells. *Blood.* 122:2550–2554.
6. Ed Rainger, G., M. Chimen, ..., G. B. Nash. 2015. The role of platelets in the recruitment of leukocytes during vascular disease. *Platelets.* 26:507–520.
7. Hitchcock, J. R., C. N. Cook, ..., A. F. Cunningham. 2015. Inflammation drives thrombosis after Salmonella infection via CLEC-2 on platelets. *J. Clin. Invest.* 125:4429–4446.
8. Watson, S. P., J. M. J. Herbert, and A. Y. Pollitt. 2010. GPVI and CLEC-2 in hemostasis and vascular integrity. *J. Thromb. Haemost.* 8:1456–1467.
9. Stalker, T. J., D. K. Newman, ..., L. F. Brass. 2012. Platelet signaling. *Handb. Exp. Pharmacol.* 59–85.
10. Gurbel, P. A., A. Kuliopulos, and U. S. Tantry. 2015. G-protein-coupled receptors signaling pathways in new antiplatelet drug development. *Arterioscler. Thromb. Vasc. Biol.* 35:500–512.
11. FitzGerald, G. A. 1991. Mechanisms of platelet activation: thromboxane A<sub>2</sub> as an amplifying signal for other agonists. *Am. J. Cardiol.* 68:11B–15B.
12. Gibbins, J. M., M. Okuma, ..., S. P. Watson. 1997. Glycoprotein VI is the collagen receptor in platelets which underlies tyrosine phosphorylation of the Fc receptor  $\gamma$ -chain. *FEBS Lett.* 413:255–259.
13. Suzuki-Inoue, K., Y. Kato, ..., Y. Ozaki. 2007. Involvement of the snake toxin receptor CLEC-2, in podoplanin-mediated platelet activation, by cancer cells. *J. Biol. Chem.* 282:25993–26001.
14. Christou, C. M., A. C. Pearce, ..., C. A. O’Callaghan. 2008. Renal cells activate the platelet receptor CLEC-2 through podoplanin. *Biochem. J.* 411:133–140.
15. Bertozzi, C. C., A. A. Schmaier, ..., M. L. Kahn. 2010. Platelets regulate lymphatic vascular development through CLEC-2-SLP-76 signaling. *Blood.* 116:661–670.
16. Suzuki-Inoue, K., O. Inoue, ..., Y. Ozaki. 2010. Essential in vivo roles of the C-type lectin receptor CLEC-2: embryonic/neonatal lethality of CLEC-2-deficient mice by blood/lymphatic misconnections and impaired thrombus formation of CLEC-2-deficient platelets. *J. Biol. Chem.* 285:24494–24507.
17. Hughes, C. E., B. A. Finney, ..., S. P. Watson. 2015. The N-terminal SH2 domain of Syk is required for (hem)ITAM, but not integrin, signaling in mouse platelets. *Blood.* 125:144–154.
18. Herzog, B. H., J. Fu, ..., L. Xia. 2013. Podoplanin maintains high endothelial venule integrity by interacting with platelet CLEC-2. *Nature.* 502:105–109.
19. Huang, T. F., C. Z. Liu, and S. H. Yang. 1995. Aggretin, a novel platelet-aggregation inducer from snake (*Calloselasma rhodostoma*) venom, activates phospholipase C by acting as a glycoprotein Ia/IIa agonist. *Biochem. J.* 309:1021–1027.
20. Shin, Y., and T. Morita. 1998. Rhodocytin, a functional novel platelet agonist belonging to the heterodimeric C-type lectin family, induces

- platelet aggregation independently of glycoprotein Ib. *Biochem. Biophys. Res. Commun.* 245:741–745.
21. Manne, B. K., T. M. Getz, ..., S. P. Kunapuli. 2013. Fucoidan is a novel platelet agonist for the C-type lectin-like receptor 2 (CLEC-2). *J. Biol. Chem.* 288:7717–7726.
  22. Boulaftali, Y., P. R. Hess, ..., W. Bergmeier. 2013. Platelet ITAM signaling is critical for vascular integrity in inflammation. *J. Clin. Invest.* 123:908–916.
  23. Hughes, C. E., L. Navarro-Núñez, ..., S. P. Watson. 2010. CLEC-2 is not required for platelet aggregation at arteriolar shear. *J. Thromb. Haemost.* 8:2328–2332.
  24. Bender, M., F. May, ..., B. Nieswandt. 2013. Combined in vivo depletion of glycoprotein VI and C-type lectin-like receptor 2 severely compromises hemostasis and abrogates arterial thrombosis in mice. *Arterioscler. Thromb. Vasc. Biol.* 33:926–934.
  25. Gros, A., V. Syvannarath, ..., B. Ho-Tin-Noé. 2015. Single platelets seal neutrophil-induced vascular breaches via GPVI during immune-complex-mediated inflammation in mice. *Blood.* 126:1017–1026.
  26. May, F., I. Hagedorn, ..., B. Nieswandt. 2009. CLEC-2 is an essential platelet-activating receptor in hemostasis and thrombosis. *Blood.* 114:3464–3472.
  27. Inoue, O., K. Hokamura, ..., Y. Ozaki. 2015. Vascular smooth muscle cells stimulate platelets and facilitate thrombus formation through platelet CLEC-2: implications in atherothrombosis. *PLoS One.* 10:e0139357.
  28. Pike, L. J. 2009. The challenge of lipid rafts. *J. Lipid Res.* 50 (Suppl):S323–S328.
  29. Payne, H., T. Ponomaryov, ..., A. Brill. 2017. Mice with a deficiency in CLEC-2 are protected against deep vein thrombosis. *Blood.* 129:2013–2020.
  30. Shirai, T., O. Inoue, ..., K. Suzuki-Inoue. 2017. C-type lectin-like receptor 2 promotes hematogenous tumor metastasis and prothrombotic state in tumor-bearing mice. *J. Thromb. Haemost.* 15:513–525.
  31. Kato, Y., M. K. Kaneko, ..., H. Narimatsu. 2008. Molecular analysis of the pathophysiological binding of the platelet aggregation-inducing factor podoplanin to the C-type lectin-like receptor CLEC-2. *Cancer Sci.* 99:54–61.
  32. O’Rafferty, C., G. M. O’Regan, ..., O. P. Smith. 2015. Recent advances in the pathobiology and management of Kasabach-Merritt phenomenon. *Br. J. Haematol.* 171:38–51.
  33. Chang, Y.-W., P. W. Hsieh, ..., C.-P. Tseng. 2015. Identification of a novel platelet antagonist that binds to CLEC-2 and suppresses podoplanin-induced platelet aggregation and cancer metastasis. *Oncotarget.* 6:42733–42748.
  34. Pollitt, A. Y., B. Grygielska, ..., S. P. Watson. 2010. Phosphorylation of CLEC-2 is dependent on lipid rafts, actin polymerization, secondary mediators, and Rac. *Blood.* 115:2938–2946.
  35. Watson, A. A., C. M. Christou, ..., C. A. O’Callaghan. 2009. The platelet receptor CLEC-2 is active as a dimer. *Biochemistry.* 48:10988–10996.
  36. Hughes, C. E., A. Y. Pollitt, ..., S. P. Watson. 2010. CLEC-2 activates Syk through dimerization. *Blood.* 115:2947–2955.
  37. Watson, A. A., J. A. Eble, and C. A. O’Callaghan. 2008. Crystal structure of rhodocytin, a ligand for the platelet-activating receptor CLEC-2. *Protein Sci.* 17:1611–1616.
  38. Pollitt, A. Y., N. S. Poulter, ..., S. P. Watson. 2014. Syk and Src family kinases regulate C-type lectin receptor 2 (CLEC-2)-mediated clustering of podoplanin and platelet adhesion to lymphatic endothelial cells. *J. Biol. Chem.* 289:35695–35710.
  39. Inoue, K., Y. Ozaki, ..., T. Morita. 1999. Signal transduction pathways mediated by glycoprotein Ia/IIa in human platelets: comparison with those of glycoprotein VI. *Biochem. Biophys. Res. Commun.* 256:114–120.
  40. Badolia, R., V. Inamdar, ..., S. P. Kunapuli. 2017. G<sub>q</sub> pathway regulates proximal C-type lectin-like receptor-2 (CLEC-2) signaling in platelets. *J. Biol. Chem.* 292:14516–14531.
  41. Mukherjee, S., J. Zhu, ..., A. Weiss. 2013. Monovalent and multivalent ligation of the B cell receptor exhibit differential dependence upon Syk and Src family kinases. *Sci. Signal.* 6:ra1.
  42. Poulter, N. S., A. Y. Pollitt, ..., S. M. Jung. 2017. Clustering of glycoprotein VI (GPVI) dimers upon adhesion to collagen as a mechanism to regulate GPVI signaling in platelets. *J. Thromb. Haemost.* 15:549–564.
  43. Dunster, J. L., A. J. Unsworth, ..., A. Y. Pollitt. 2020. Interspecies differences in protein expression do not impact the spatiotemporal regulation of glycoprotein VI mediated activation. *J. Thromb. Haemost.* 18:485–496.
  44. Dunster, J. L., F. Mazet, ..., M. J. Tindall. 2015. Regulation of early steps of GPVI signal transduction by phosphatases: a systems biology approach. *PLoS Comput. Biol.* 11:e1004589.
  45. Sveshnikova, A. N., A. V. Balatskiy, ..., M. A. Pantelev. 2016. Systems biology insights into the meaning of the platelet’s dual-receptor thrombin signaling. *J. Thromb. Haemost.* 14:2045–2057.
  46. Gillespie, D. T. 2007. Stochastic simulation of chemical kinetics. *Annu. Rev. Phys. Chem.* 58:35–55.
  47. Dunster, J. L., M. A. Pantelev, ..., A. N. Sveshnikova. 2018. Mathematical techniques for understanding platelet regulation and the development of new pharmacological approaches. *Methods Mol. Biol.* 1812:255–279.
  48. Mazurov, A. V., D. V. Vinogradov, ..., V. N. Smirnov. 1991. A monoclonal antibody, VM64, reacts with a 130 kDa glycoprotein common to platelets and endothelial cells: heterogeneity in antibody binding to human aortic endothelial cells. *Thromb. Haemost.* 66:494–499.
  49. Pantelev, M. A., N. M. Ananyeva, ..., E. L. Saenko. 2005. Two subpopulations of thrombin-activated platelets differ in their binding of the components of the intrinsic factor X-activating complex. *J. Thromb. Haemost.* 3:2545–2553.
  50. Gibbins, J. M. 2004. Study of tyrosine kinases and protein tyrosine phosphorylation BT. In *Platelets and Megakaryocytes: Volume 2: Perspectives and Techniques*. J. M. Gibbins and M. P. Mahaut-Smith, eds. Humana Press, pp. 153–167.
  51. Mahammad, S., and I. Parmryd. 2015. Cholesterol depletion using methyl- $\beta$ -cyclodextrin. *Methods Mol. Biol.* 1232:91–102.
  52. Lawrence, M. B., L. V. McIntire, and S. G. Eskin. 1987. Effect of flow on polymorphonuclear leukocyte/endothelial cell adhesion. *Blood.* 70:1284–1290.
  53. Pahle, J. 2009. Biochemical simulations: stochastic, approximate stochastic and hybrid approaches. *Brief. Bioinform.* 10:53–64.
  54. Balabin, F. A., and A. N. Sveshnikova. 2016. Computational biology analysis of platelet signaling reveals roles of feedbacks through phospholipase C and inositol 1,4,5-trisphosphate 3-kinase in controlling amplitude and duration of calcium oscillations. *Math. Biosci.* 276:67–74.
  55. Séverin, S., A. Y. Pollitt, ..., S. P. Watson. 2011. Syk-dependent phosphorylation of CLEC-2: a novel mechanism of hem-immunoreceptor tyrosine-based activation motif signaling. *J. Biol. Chem.* 286:4107–4116.
  56. Manne, B. K., R. Badolia, ..., S. P. Kunapuli. 2015. Distinct pathways regulate Syk protein activation downstream of immune tyrosine activation motif (ITAM) and hemITAM receptors in platelets. *J. Biol. Chem.* 290:11557–11568.
  57. Fuller, G. L. J., J. A. E. Williams, ..., A. C. Pearce. 2007. The C-type lectin receptors CLEC-2 and Dectin-1, but not DC-SIGN, signal via a novel YXXL-dependent signaling cascade. *J. Biol. Chem.* 282:12397–12409.
  58. Bradshaw, J. M. 2010. The Src, Syk, and Tec family kinases: distinct types of molecular switches. *Cell. Signal.* 22:1175–1184.
  59. Tsang, E., A. M. Giannetti, ..., J. M. Bradshaw. 2008. Molecular mechanism of the Syk activation switch. *J. Biol. Chem.* 283:32650–32659.
  60. Manne, B. K., R. Badolia, ..., S. P. Kunapuli. 2015. C-type lectin like receptor 2 (CLEC-2) signals independently of lipid raft microdomains in platelets. *Biochem. Pharmacol.* 93:163–170.

61. Baba, Y., and T. Kurosaki. 2011. Impact of Ca<sup>2+</sup> signaling on B cell function. *Trends Immunol.* 32:589–594.
62. Sveshnikova, A. N., F. I. Ataullakhanov, and M. A. Panteleev. 2015. Compartmentalized calcium signaling triggers subpopulation formation upon platelet activation through PAR1. *Mol. Biosyst.* 11:1052–1060.
63. Burkhart, J. M., M. Vaudel, ..., R. P. Zahedi. 2012. The first comprehensive and quantitative analysis of human platelet protein composition allows the comparative analysis of structural and functional pathways. *Blood.* 120:e73–e82.
64. Filkova, A. A., A. A. Martyanov, ..., A. N. Sveshnikova. 2019. Quantitative dynamics of reversible platelet aggregation: mathematical modelling and experiments. *Sci. Rep.* 9:6217.
65. Jiang, P., S. Loyau, ..., M. Jandrot-Perrus. 2015. Inhibition of glycoprotein VI clustering by collagen as a mechanism of inhibiting collagen-induced platelet responses: the example of losartan. *PLoS One.* 10:e0128744.
66. Robinson, P. K. 2015. Enzymes: principles and biotechnological applications. *Essays Biochem.* 59:1–41.
67. Struvay, C., and G. Feller. 2012. Optimization to low temperature activity in psychrophilic enzymes. *Int. J. Mol. Sci.* 13:11643–11665.
68. Medda, L., M. Monduzzi, and A. Salis. 2015. The molecular motion of bovine serum albumin under physiological conditions is ion specific. *Chem. Commun. (Camb.)* 51:6663–6666.
69. Saha, S., I.-H. Lee, ..., S. Mayor. 2015. Diffusion of GPI-anchored proteins is influenced by the activity of dynamic cortical actin. *Mol. Biol. Cell.* 26:4033–4045.
70. Kardeby, C., K. Fälker, ..., M. Grenegård. 2019. Synthetic glycopolymers and natural fucoidans cause human platelet aggregation via PEAR1 and GPIb $\alpha$ . *Blood Adv.* 3:275–287.
71. Alshehri, O. M., S. Montague, ..., S. P. Watson. 2015. Activation of glycoprotein VI (GPVI) and C-type lectin-like receptor-2 (CLEC-2) underlies platelet activation by diesel exhaust particles and other charged/hydrophobic ligands. *Biochem. J.* 468:459–473.